sustainability

MDPI

Article

Modeling Pedestrian Detour Behavior By-Passing Conflict Areas

Qingyan Ning [1,*] and Maosheng Li [1,2]

[1] School of Traffic and Transportation Engineering, Central South University, Changsha 410075, China
[2] Rail Data Research and Application Key Laboratory of Hunan Province, Central South University, 22 South Shaoshan Road, Changsha 410075, China
* Correspondence: qingyanning@csu.edu.cn

Abstract: In the process of walking, most pedestrians prefer to choose the shortest path, which requires passing through the conflict area. However, in the case of high crowd density, 5–20% of the total population will choose to follow the pre-planned route before walking or during the initial period of the trip to bypass the conflict area. Aiming at reproducing this detour behavior phenomenon, an extended social force model (SFM) is proposed according to a three-layer pedestrian simulation framework. This model not only fully considers the choice of detour mode, but also contains the avoidance and game behavior at the conflict point. At the strategic layer, a detour mode selection model based on the Logit model is established considering the pedestrian starting time and detour angle, to distinguish between the two groups of pedestrians who follow the pre-planned route and those who repeatedly adjust the route during the trip. Then, the path decision based on visual perception density at the tactical layer and the Voronoi-based SFM at the operational layer are combined to guide the specific movement of the two types of pedestrian groups. A series of evaluation indexes such as the central density, the mean local density, and detour level is selected, and Kolmogorov–Smirnov (K-S) test and dynamic time warping (DTW) method are used to evaluate and compare the scores of each index of different models. The results show that the model can improve the existing pedestrian detour simulation model to a certain extent. In sum, the travel time score, the detour level, and the mean local density score respectively increase from 0.71 to 0.81, 0.46 to 0.81, and 0.39 to 0.48, which indicates a significant improvement in walking performance.

Keywords: pedestrian dynamics; detour behavior; social force model; perceptual density; heuristic rules

Citation: Ning, Q.; Li, M. Modeling Pedestrian Detour Behavior By-Passing Conflict Areas. *Sustainability* **2022**, *14*, 16522. https://doi.org/10.3390/su142416522

Academic Editors: Shuchao Cao, Xiaomeng Shi and Mohcine Chraibi

Received: 2 October 2022
Accepted: 6 December 2022
Published: 9 December 2022

1. Introduction

With the continuous growth of the urban population and the continuous emergence of large-scale public infrastructure, the research on pedestrian dynamics has become more and more important due to tasks such as formulating crowd evacuation strategies [1] and optimizing building structure design [2]. Pedestrian movement behavior is an important research direction of pedestrian dynamics, which has a serious impact on the spatial distribution density of pedestrians and the flow on different walking paths. The research on pedestrian movement behavior has attracted the attention of many researchers. For pedestrian movement behavior, existing models are mainly divided into macroscopic models and microscopic models according to the underlying spatial resolution and crowd size. Macroscopic models mainly simulate the behavior and mobility of the whole population, while ignoring individual behavior. Common macro models include the continuum model [3], the network model [4], and the hybrid model [5]. Microscopic models simulate smaller groups and take into account the more detailed behavior of individuals in the group. Common microscopic models include cellular automata model (CA) [6,7], social force model (SFM) [8,9], velocity obstacle model (VO) [10,11], and discrete choice model (DCM) [12]. Compared with the macroscopic model, the microscopic model can better represent the individual response, so it is often used in the study of individual movement behavior. As the SFM can well reflect the real situation of pedestrian movement and reproduce many pedestrian self-organization phenomena, it has been widely used in the simulation and modeling of pedestrian flow. In the past few decades, various model modifications have been proposed based on the traditional social force model (SFM). According to the different psychology of pedestrians in the process of movement, most simulation frameworks based on SFM start from three layers of pedestrian decision-making, namely, the strategical layer describing pedestrian activity plans, the tactical layer describing pedestrian route choices, and the operational layer describing the competitive game behavior among pedestrians [13]. Focusing on the operational layer, pedestrians decide the travel speed and direction to take immediately in the next step. Farina et al. [14] incorporated the pedestrian travel direction into the SFM to reflect the lateral motion of pedestrians; Li et al. [15] improved the SFM by considering the difference in pedestrian speed and self-driving force down the escalator. In addition to immediate action, pedestrians need to decide where to take action based on their understanding of the environment and personal preferences, which is the goal achieved at the tactical level. Moussaid et al. [16] proposed two simple heuristic rules to describe avoidance behavior; Yuen and Lee [17] focused on the phenomenon that pedestrians with high speed are accustomed to overtaking pedestrians with low speed, and modified the SFM to reflect the overtaking behavior of pedestrians. Pedestrians are complex individuals, and any continuous behavioral process can be divided into pre-travel (strategic) and in-travel (tactical and operational). Hoogendoorn et al. [18] proposed a multi-class continuum model on the basis of the microscopic SFM, describing the pedestrian global path choice before walking at the strategic level and the pedestrian local path choice during the trip at the tactical level. It realized the three-layer pedestrian motion modeling at the strategic level, the tactical level, and the operation level. Modeling based on the three-layer level can not only reveal the competitive game behavior between pedestrians but also show the ability of pedestrians to avoid high-density areas.

Detour behavior is an important characteristic during pedestrian motion, especially in conflict scenarios. It has an important effect on the efficiency of crowd evacuation. At the same time, the exploration of detour routes will help urban managers better layout public facilities. In the study of detour behavior, Xiao et al. [19] determined the pedestrian detour direction, following direction according to the Voronoi diagram; Qu et al. [20] applied the Voronoi diagram to improve the SFM to better describe the detour behavior of pedestrians. These studies only describe the pedestrian immediate responses to conflict at the operational level and lack the impact of global navigation decisions. In order to make up for this defect, Li et al. [21] proposed a two-layer detour decision model based on perception density. In this model, Pedestrians can predict the path points according to the crowding degree in the visual field, so as to guide the operational layer to make detour decisions in advance. The research shows that adding guidance at the tactical layer makes pedestrian detour behavior more reasonable. Generally speaking, crowds are always composed of heterogeneous pedestrians. When facing the same walking space, they have different movement behaviors. However, the above research only describes the movement behavior of pedestrians who repeatedly adjust their routes during the trip and does not take into account the different path selection modes of some pedestrians, that is, some pedestrians bypass the conflict area directly and choose large detours before walking or during the initial period of the trip. This makes the pedestrian density in the simulation much higher than the actual density.

In response to this problem, this study improves and expands the existing model at the strategic level, and proposes an extended SFM that not only fully considers the path selection mode, but also includes the avoidance game behavior at the conflict point of pedestrian travel routes. There are two ways for pedestrians to move from one place to another. One is to follow a pre-planned route to avoid the conflict zone. The study found that: in the case of high crowd density, this part of the population can account for 5%–20%. This ratio is related to the degree of crowding, but there is no doubt that it has an important impact on the overall movement of the group. Another is to go through the conflict zone and adjust the route repeatedly to pursue the shortest path to reach the destination. Studies have found that personal preference [22], and sensitivity to comfort and safety [19] are the main factors that affect the detour decision-making of pedestrians. Especially in the case of high crowd density, the proportion of following a pre-planned route to avoid the conflict zone will increase significantly. Therefore, it is necessary to distinguish groups who choose two different path selection modes. At the strategic level, the Logit model is used to separate the two groups. At the tactical level, pedestrian detour paths are predicted by Voronoi-based perceptual density in the pedestrian visual field. It should be noted that the group that repeatedly adjust the routes during the trip will always consider the distance to the destination point more important, while the group that follows the pre-planned route only considers the comfort of walking priority before bypassing the conflict area. At the operational layer, the target direction is set according to the path direction, which is determined by the tactical layer, and the SFM is used to guide the specific movement of pedestrians. In the simulation, evaluation indexes such as travel time, pedestrian density are extracted, and the dynamic time warping (DTW) method and Kolmogorov–Smirnov (K-S) test are used to test and evaluate the similarity of different indicators between simulation and experiment. The results show that the extended SFM model is more similar to the real scene in the presentation and distribution of pedestrians in the walking space than the previous detour model, and the scores of the three indexes of travel time, detour level, and mean local density are significantly improved.

The rest of the paper is organized as follows. The Section 2 introduces the pedestrian detour decision model based on the strategic, tactical, and operational layers. Section 3 analyzes the experimental data to select evaluation indicators and reflect the detour characteristics. Section 4 conducts simulation experiments to evaluate the model. Finally, the conclusions are summarized in Section 5.

2. Model

This section presents a three-layer framework for pedestrian detour behavior, as shown in Figure 1. First, at the strategic level, it corresponds to the environmental cognition and response time before walking or during the initial period of the trip. At this time, pedestrians will make macro decisions conducive to their subsequent walking. Based on this idea, a Logistic regression model (Logit model) is established to predict the pedestrian detour mode choice. It should be noted that the strategical layer determines the detour mode of pedestrians before walking, rather than the choice of departure time and destination, which is slightly different from the strategical layer proposed by Hoogendoorn and Bovy [13]. However, Hoogendoorn classified pre-trip behavior as a strategic layer in references (Hoogendoorn et al. [23]), so we think this mode choice belongs to a strategic layer choice.

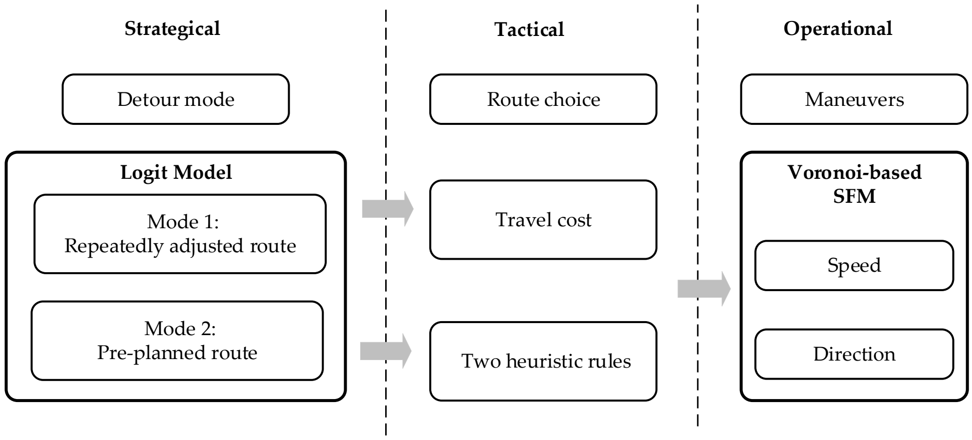

Figure 1. The simplified three-layer framework for pedestrian detour behavior.

At the tactical and operational levels, for one detour mode (repeatedly adjusting the route during the trip), the detour decision model proposed by Li et al. [21] will be briefly reviewed; for another detour mode (pre-planning the route), two heuristic rules are set based on perceived density to make waypoint decisions. Therefore, an extended SFM is established that not only fully considers the choice of the detour mode, but also contains the avoidance and game behavior at the conflict point of the travel route. Pedestrian detour mode, detour direction, and specific detour behavior are described in detail in Section 2.1, Section 2.2, Section 2.3 respectively.

2.1. Strategic Layer Model

In the circle antipode walking experiment, there is a common conflict area since each pedestrian walks to the symmetrical point. As shown in the area enclosed by the white circle in the center of Figure 2a, the brighter the color, the greater the repulsive force on pedestrians. Here, the repulsive force is calculated by the repulsive formula of the SFM, i.e., F_{ij}^{R} in Equation (12). The repulsive force can reflect the conflict between pedestrians, and the greater the repulsive force, the more obvious the conflict between pedestrians. When the conflict reaches a certain degree, pedestrians will make a decision in advance between choosing the shortest path (e.g., route 1) in Region 1 and choosing a comfortable route (e.g., route 2) to avoid conflict in Region 2. In order to get a comfortable walking experience, a small number of pedestrians will pre-plan the route and directly choose large detours, or even walk along the scene boundary (e.g., route 3).

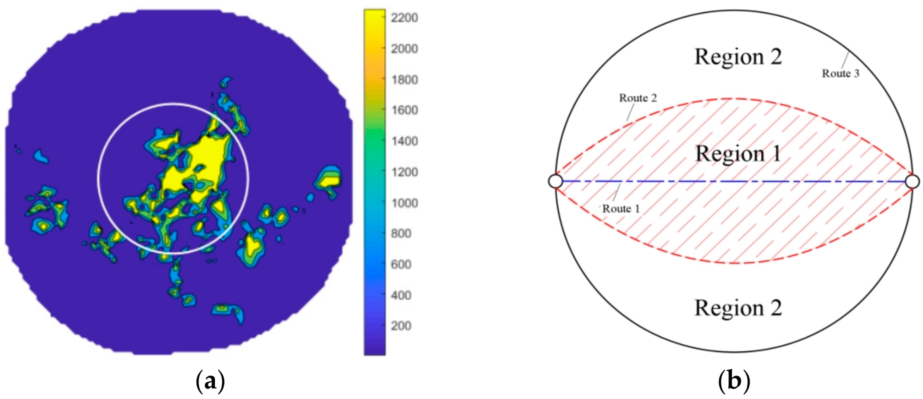

Figure 2. Pedestrian common conflict area and the corresponding three routes. (**a**) Common conflict area, (**b**) different route choices.

In order to distinguish the two detour modes between Region 1 and Region 2, Logit model is used to divide pedestrians into two groups: "repeatedly adjusting the route during the trip" and "pre-planning the route before walking or during the initial period of the trip". Since the situation of walking along the scene boundary is not common, this paper does not consider this situation separately.

Logit model is one of the classical discrete choice models. When people are faced with two or more choices (such as waiting or moving, buying, or not buying), logit model can reflect the choice probability, and the solution speed is fast. In addition, when each variable changes, Logit model can easily solve the selected probability of each choice in the new environment. It is widely used in transportation [24], marketing [25], and evacuation [26]. In this model, the pedestrian detour mode is regarded as a binary dependent variable y_i. $y_i = 0$ represents the mode of repeatedly adjusting the route during the trip; $y_i = 1$ represents the mode of pre-planning the route before walking or during the initial period of the trip. There are many factors affecting the choice of detour mode, such as age, gender, physical condition, whether there is heavy luggage, road conditions and other factors. In this experiment scenario, the experimenter is 18–28 years old, in good health, and energetic. The test site is flat and free of water, which can provide greater friction force. These influencing factors are relatively consistent in the experiment, which is not considered in this study. In this paper, detour angle X_1 and pedestrian starting time X_2 are regarded as independent variables. The Logit model is established as follows:

$$p_i(y_i = 1|(X_1, X_2)) = \frac{\exp(a + \sum_{i=1}^{n} b_i X_i)}{1 + \exp(a + \sum_{i=1}^{n} b_i X_i)} \tag{1}$$

Here, a is a constant term; b_i is the regression coefficient, representing the correlation between independent variable and dependent variables; X_i stands for independent variable, where X_1 is the detour angle and X_2 is starting time.

2.2. Tactical Layer Model

Pedestrians can adjust their path direction according to visual information [12]. The visual field of pedestrian P_i takes the direction of the target point as the center. The visual angle is $[-\Phi, \Phi]$ and the visual length is L, as shown in Figure 3. The visual field is divided into $2M$ sub-areas, which are marked as $VR_i = \left\{A_{i_1}, \cdots, A_{i_n}, \cdots, A_{i_{2M}}\right\}(n = 1, 2, \ldots, 2M)$. The corresponding path points are distributed on the middle points of the sub-areas, and the set of path points is $\left\{DP_{i_1}, \cdots, DP_{i_n}, \cdots, DP_{i_{2M}}\right\}$. In addition, the path point index less than M is the path point of the pedestrian group that repeatedly adjusts routes during the trip, as shown in the blue area in Figure 3, otherwise, it is the path point of the pedestrian group that directly chooses large detours.

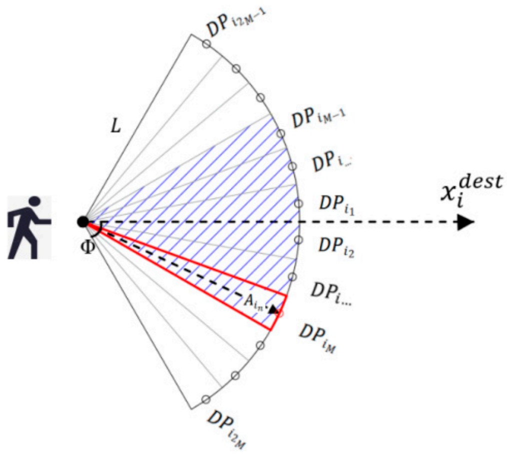

Figure 3. The pedestrian visual field and the constantly adjust routes area.

In the walking process, pedestrians P_i will predict the crowded area and degree after $t_i = L/v_i^{des}$ moment, so as to adjust the walking direction. In addition, due to different desired speeds, pedestrians have different perceived density of the visual field. Taking A_{i_n} (the area enclosed by the bold red line in Figure 3) as an example, the perceived density of the sub-area is:

$$D_{A_{i_n}}(t + t_i) = \begin{cases} \frac{p_{A_{i_n}}(x_i)}{|A_{i_n}|} \cdot \frac{v_i}{v_i^{des}}; & if A_{i_n} \in Set(S) \\ \frac{p_{A_{i_n}}(x_i)}{|A_{i_n}|}; & otherwise \end{cases} \tag{2}$$

Here, $|A_{in}|$ is the size of A_{in}, v_i is the current speed of P_i, v_i^{des} is the desired speed, $Set(S)$ is the set of visual sub-sectors where the path point index is less than M, and $p_{A_{in}}(x_i)$ is the pedestrian density calculated by the Voronoi diagram.

The pedestrian density $p_{A_{in}}(x_i)$ use Voronoi cells size formed by pedestrian movements to reflect the density of the region, which is proposed by Steffen and Seyfried [27].

All Voronoi cells in the region A_{i_n} are used to calculate the density of this region $p_{A_{in}}(x_i)$, see Equation (3)

$$p_{A_{i_n}}(x_i) = \sum_i \frac{1}{|V_i|}, \quad A_{i_n} \cap V_i \neq 0, \ \forall i \tag{3}$$

Here, x_i is the position of P_i, V_i is the Voronoi cell of P_i, and $|V_i|$ is the size of the Voronoi cell V_i.

2.2.1. Group That Repeatedly Adjust Routes during the Trip

For pedestrians who constantly adjust their routes, they consider the density of A_{in} and the distance between the corresponding path points and the destination point in order to pursue the shortest route. The definition of travel cost E_{i_n} is consistent with the reference Li et al. [21].

$$E_{i_n} = \left(k_1 \cdot \frac{\|DP_{i_n} - x_i^{dest}\|}{\sum_{n=1}^{2M} \|DP_{i_n} - x_i^{dest}\|} + k_2 \cdot \frac{D_{A_{i_n}}(t+t_i)}{\sum_{n=1}^{2M} D_{A_{i_n}}(t+t_i)} \right) \tag{4}$$

Here, DP_{in} is the path point in the visual field of P_i, x_i^{dest} is the destination position of P_i. k_1 and k_2 are the weight parameters.

Furthermore, considering the right-side avoidance rule [28], the minimum travel cost of left and right routes is calculated as follows:

$$DP_{i_l} = argmin\left(E_{i_{n'}}\right), n' = 1, 3, \cdots, M-1 \tag{5}$$

$$DP_{i_r} = argmin\left(E_{i_{n''}}\right), n'' = 2, 4, \cdots, M \tag{6}$$

If DP_{i_l} minus DP_{i_r} is less than or equal to the given right tendency threshold δ, the pedestrian will detour toward the right path point, see Equation (7).

$$DP_* = \begin{cases} DP_{i_r}, & \text{if } DP_{i_r} - DP_{i_l} \leq \delta \\ DP_{i_l}, & \text{otherwise} \end{cases} \tag{7}$$

2.2.2. Group That Pre-Plan Route before Walking or during the Initial Period of the Trip

Some pedestrians who pursue comfortable routes pre-plan the detour route before walking or during the initial period of the trip, that is, they completely avoid the common conflict area and directly choose large detours. They hope to move freely without too much interference [3,29]. Therefore, two heuristic rules are proposed.

The first rule is that pedestrians will set intermediate navigation points in the path [30] and in the process of moving toward the intermediate position, pedestrians pay more attention to the comfort of the journey.

Guided by this rule, the intermediate navigation point is simply set on the vertical bisector of the line connecting the start and destination points. In the process of moving toward the middle navigation point, the path selection area is shown in the blue area in Figure 4, the left and right detour path point is determined by Equations (8) and (9). Similarly, consider the right-hand tendency of pedestrians, see Equation (7).

$$DP_{i_l} = argmin\left(D_{A_{in'}}(t+t_i)\right), n' = M+1, M+3\cdots, 2M-1 \tag{8}$$

$$DP_{i_r} = argmin\left(D_{A_{in''}}(t+t_i)\right), \ n'' = M+2, \cdots, 2M \tag{9}$$

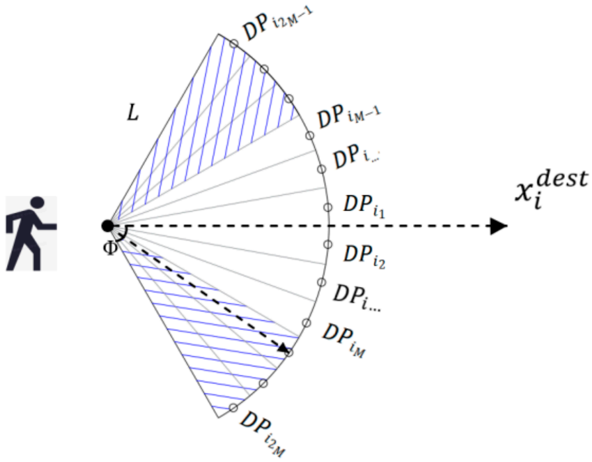

Figure 4. Schematic diagram of large-scale detour area.

The second rule is that pedestrians pay more attention to the distance from the target point when crossing the middle position to the target point. This reflects the straightness of pedestrians walking toward the target point. So, the optimal path point is:

$$DP_* = x_i^{dest} \tag{10}$$

After determining the path point DP_*, the optimal path direction $\overrightarrow{e}^{\text{path}}$ of the two groups of "repeatedly adjusting the route during the trip" and "pre-planning the route before walking or during the initial period of the trip" can be unified into Equation (11).

$$\overrightarrow{e}^{\text{path}} = (DP_* - x_i) / \|DP_* - x_i\| \tag{11}$$

2.3. Operational Layer Model

2.3.1. Movement Speed

Social force model (SFM) is a classic pedestrian motion model based on Newtonian mechanics, see Equation (12). The motion of each pedestrian is affected by three kinds of forces, namely, self-driving force F_i^D, the repulsive force by other pedestrians F_{ij}^R, and the repulsive force by obstacles F_{iW}^O. Therefore, the change of pedestrian walking speed can be determined according to Newton's second law. More details can be found in the reference(Helbing [8]).

$$m_i \frac{dv_i(t)}{dt} = F_i^D + F_{ij}^R + F_{iW}^O \tag{12}$$

In SFM, pedestrians are driven by the combined force of self-driving force, the repulsive force between pedestrians, and the force between pedestrians and obstacles. In other words, pedestrians move isotropically. When the pedestrian density in the scene is large, the interaction between pedestrians will lead to pedestrian movement blocks or stagnation. Empirical evidence shows that most of the time, pedestrians tend to move forward, that is, their speed vector is usually consistent with their direction [14]. Therefore, the correction of motion speed is shown in Equation (13). If the angle between the speed direction and the desired speed direction is greater than 90°, the pedestrian will choose to stop moving temporarily, and the pedestrian's speed is 0. This functional form was chosen just because it is the simplest self-stopping mechanism that reproduces the experimental trajectory [31], as shown in Section 4.

$$v_i(t) = \begin{cases} v_i(t), & \text{if } \overrightarrow{e}_i^{v} \cdot \overrightarrow{e}_i^{desire} \geq 0 \\ 0, & otherwise \end{cases} \tag{13}$$

2.3.2. Movement Direction

For pedestrians P_i, the desired direction points to the optimal path direction, which depends on the tactical layer described above:

$$\vec{e}_i^{\,dest} = \vec{e}_i^{\,\text{path}} \tag{14}$$

In the process of walking toward $\vec{e}_i^{\,dest}$, pedestrian shall deal with the local conflict with the pedestrian in front and move toward the local detour direction [32]. Thus, the desired direction can be determined by Equation (15).

$$\vec{e}_i^{\,desire} = \begin{cases} \vec{e}_i^{\,dest}, & C \geq 0 \\ \vec{e}_i^{\,dtr}, & otherwise \end{cases} \tag{15}$$

C is a judgment variable, see Equation (16). The choice of pedestrian walking toward the path direction or the local detour direction is determined by the conflict with the front pedestrian P_f. If $C < 0$, pedestrian P_i may collide with P_f within relaxation time τ_i.

$$C = d_{if} - \beta \cdot \tau_i \left(v_i * \vec{e}_i^{\,v} - v_f * \vec{e}_i^{\,f} \right) \vec{n}_{if} \tag{16}$$

Here, d_{if} is the distance from P_i to P_f; β is a constant parameter; τ_i is the relaxation time of P_i; v_i and v_f are the velocity values of pedestrian P_i and P_f; $\vec{e}_i^{\,v}$ and $\vec{e}_i^{\,f}$ are the velocity directions of P_i and P_f; $\vec{n}_{if}$ is the unit vector direction pointing from P_i to P_f.

$\vec{e}_i^{\,dtr}$ is the optimal local detour direction. Considering the local Voronoi-based density and the conflict with the pedestrians in front, it is defined as the direction pointing to the Voronoi node. More details can be found in the reference (Xiao et al. [32]).

3. Experimental Data Analysis

In this section, the circle antipode walking experiment and some evaluation indexes of the model are briefly introduced. At the same time, the two detour modes, starting time, and detour angle in the experiment are analyzed to reflect the detour characteristics of pedestrians.

3.1. Experiment Setting

Controlled laboratory experiment is one of the methods used and studied in the current empirical research. It refers to the actual pedestrian movement research under non-emergency conditions with pedestrians as the research subject and pedestrians or movement environment with certain designs or restrictions. Although it is not a completely real and natural pedestrian movement, the pedestrian movement in the experiment is enough to reflect most of the pedestrian behavior in real pedestrian movement.

In 2017, Jiang Rui and other scholars from Beijing Jiaotong University carried out the circle antipode walking experiment. The experiment has been fully described in references Xiao et al. [32], and only a brief introduction is given here. The experiment is divided into two types with circle radii of 5 m and 10 m. Each person's starting position and antipode position are uniformly assigned a mark with the same number, as shown in Figure 5. Experiments with a radius of 5 m and 10 m included 8, 16, 32, and 64 participants respectively. For convenience, the 5 m experiment with 32 participants is named 5m-32p. Taking the 5m-32p experiment as an example, half of the participants were assigned a number from 1 to 16, which means that two people have the same number. After receiving the start command, all pedestrians need to walk to the same number position. All participants are 18–28 years old students from Beijing Jiaotong University. They did not wear uniforms, but all participants were required to wear clothes that are not bright.

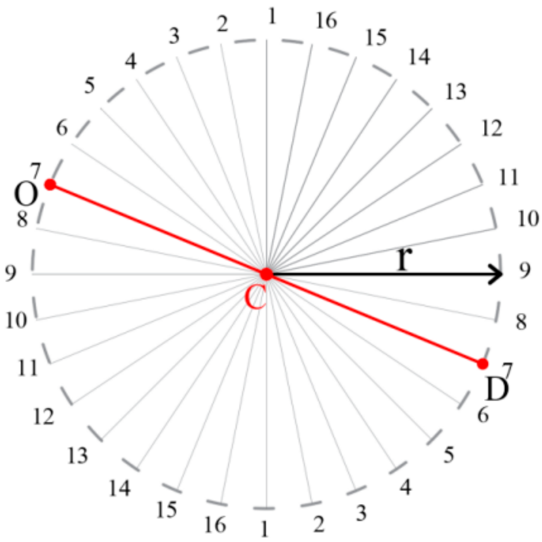

Figure 5. Scene diagram of the circle antipode experiment.

Video of the experiment was recorded with a high-definition camera and Petrack software was used to extract experimental data. In the visual presentation of the data, we recorded the walking trajectory and rotation trajectory of each pedestrian. Rotational trajectory refers to the starting and ending points of all pedestrians being rotated to the same point respectively.

3.2. Model Evaluation Indexes

The original trajectory constitutes the data source of quantitative analysis. The trajectory data of pedestrians in the walking experiment can be expressed by Equation (17):

$$s_i(t) = \left\{ \left((x_i(t), y_i(t)) \middle| 1 \le i \le N, t_i^{start} \le t \le t_i^{dest} \right) \right\} \tag{17}$$

Here, $x_i(t)$, $y_i(t)$ are the coordinates of P_i. t_i^{start} is the departure time of P_i, t_i^{dest} is the arrival time of P_i.

In addition, in order to show the pedestrian's path detour decision and conflict avoidance characteristics more intuitively, rotate the original path trajectory around the center of the circle until the starting point of the path overlaps with point O, as shown in Figure 6. The pedestrian polar coordinate after rotation is calculated by Equation (20):

$$(\rho, \theta) = \begin{cases} \left(\sqrt{(x_i(t))^2 + (y_i(t)^2)}, \arctan\frac{y_i(t)}{x_i(t)} - \arctan\frac{y_i(0)}{x_i(0)} + pi \right) & \text{if } \arctan\frac{y_i(t)}{x_i(t)} \ge 0 \\ \left(\sqrt{(x_i(t))^2 + (y_i(t)^2)}, \arctan\frac{y_i(t)}{x_i(t)} + 2pi - \arctan\frac{y_i(0)}{x_i(0)} + pi \right) & \text{if } \arctan\frac{y_i(t)}{x_i(t)} < 0 \end{cases} \tag{18}$$

textls[-25]Then, the polar coordinates are converted into rectangular coordinates, i.e., $(\rho \sin\theta, \rho\cos\theta)$. The rotated pedestrian trajectory data are represented by Equation (19):

$$s_i^R(t) = \left\{ \left(\left(x_i^R(t), y_i^R(t) \right) \middle| 1 \le i \le N, t_i^{start} \le t \le t_i^{dest} \right) \right\} \tag{19}$$

In order to evaluate the accuracy of the simulation model in reproducing the actual pedestrian behavior, a series of statistical indicators are used to analyze the experimental and simulation data.

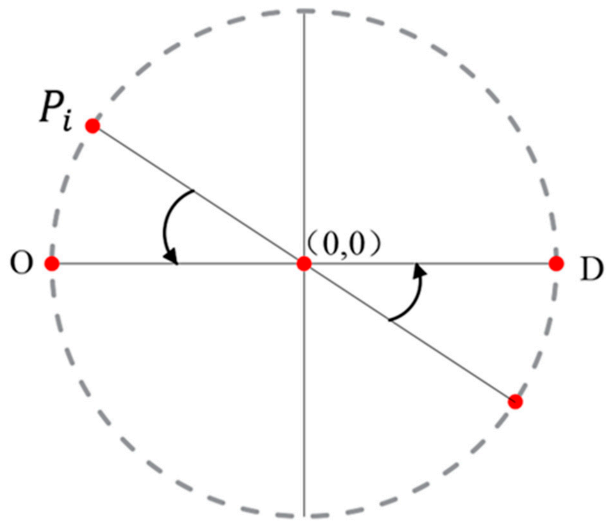

Figure 6. Pedestrian trajectory rotation in the circle antipode experiment.

Travel time: The time for pedestrians to walk from the departure point to the destination point, see Equation (20).

$$T_i = t_i^{dest} - t_i^{start} \quad (20)$$

Route length: The route length L_i of P_i is calculated according to Equation (21) based on the original trajectory.

$$L_i = \sum_{t=t_i^{start}}^{t_i^{dest}-1} \| s_i(t+1) - s_i(t) \| \quad (21)$$

Detour level: It intuitively shows the degree of pedestrians bypassing crowded areas, see Equation (22).

$$D_i = \frac{L_i \cdot M_i}{L_i^0 \cdot L_i^0} \quad (22)$$

Here, $l_i^0 = 2r$, r is the experiment radius; M_i is the route potential calculated by Equation (23):

$$M_i = \sum_{t=t_i^{start}}^{t_i^{dest}-1} \left(\frac{y_i^R(t+1) + y_i^R(t)}{2} \cdot \left(x_i^R(t+1) - x_i^R(t) \right) \right) \quad (23)$$

Density time series: Two indexes of the central area density and the mean local density are selected to explore the density characteristics of pedestrian detours. The calculation areas are $2 \times 2 = 4\ \mathrm{m}^2$ and $12 \times 12 = 144\ \mathrm{m}^2$ square areas centered on the experimental center. The density is calculated by Equation (3).

3.3. Detour Statistical Characteristics

3.3.1. Starting Time

In order to reflect the different initial situations of pedestrians after receiving the walking command, the concept of starting time is introduced, which is defined as the interval between the travel time of the first 1 m and the time of receiving the walking command. The calculation is shown in Equation (24):

$$T_{1i} = t_i^{1m} - \min\left(t_i^{start}\right) \quad (24)$$

Here, t_i^{1m} is the travel time of the first 1 m. $\min\left(t_i^{start}\right)$ is the earliest pedestrian start time, which is equivalent to the time of receiving the walking command.

The distribution of pedestrian starting time in each experiment is shown in Figure 7. The average starting time increases with the increase of the number of pedestrians. That is because the increase in the number of pedestrians makes the intersection path area more crowded, and pedestrians need more time to make trade-off decisions in high-density scenes. In the 5 m experiments, the starting time is in the range of 5~50 frames, and the interval time of each frame is 0.04 s. In the 10 m experiments, the starting time is in the range of 5~30 frames. Each distribution has a peak, which increases with the increase of the number of pedestrians. K-S test is used to test whether the distribution of starting time conforms to normal distribution, as shown in Table 1. The *p*-value refers to the probability when the assumption is true. When *p*-value is greater than 0.05, it indicates that there is no significant difference between the distribution of starting time and the normal distribution, that is, the starting time obeys the normal distribution at the confidence level of 0.05.

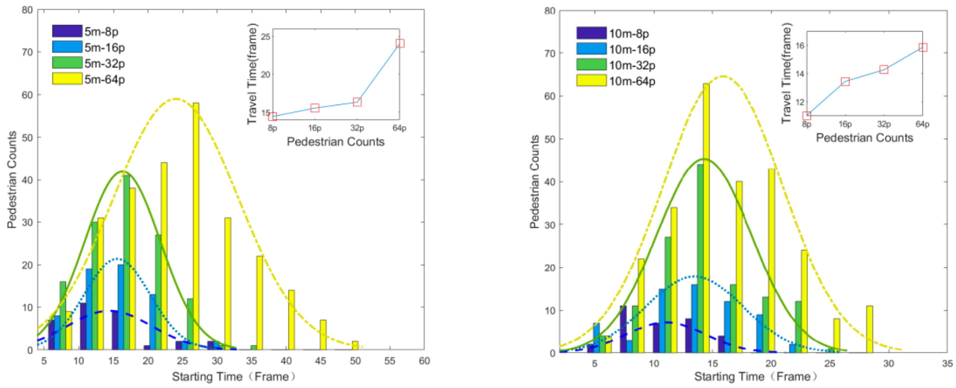

Figure 7. The distribution of pedestrian starting time.

Table 1. The *p*-value of the pedestrian starting time.

Experiment	*p*-Value			
	8p	16p	32p	64p
5 m	0.4288	0.6495	0.3389	0.1354
10 m	0.1411	0.1376	0.6501	0.5860

3.3.2. Detour Mode and Angle

Facing the central conflict area, pedestrians will choose different detour modes. This paper divides pedestrians into two groups: "repeatedly adjusting the route during the trip" and "pre-planning the route before walking or during the initial period of the trip". For P_i, when his or her route deviates from the shortest route by more than 45%, it is classified as a group that chooses a large detour by following the pre-planned route before or during the initial period of the trip (Route 1), otherwise, it is a group that repeatedly adjusts the route during the walking process (Routes 2 and 3). Analyzing the trajectory data, a comparison chart of the proportion of detour modes in each experiment is obtained, which is shown in Figure 8.

In Figure 8, Routes 1, 2, and 3 are consistent with those described in Figure 2b. Among them, Route 3 is a special case in the latter group. We can see that the proportion of pedestrians choosing large detours (Route 2) increases gradually in the 5 m experiments, and the proportion at 5m-32p is close to 20%. Moreover, when the number of pedestrians reaches 64, the proportion of pedestrians walking around the boundary increases significantly, this is due to excessive pedestrian congestion. In the 10 m experiments, the proportion of this large detour (Route 2) is low. At 10m-64p experiment, the proportion is close to 10%, less than 5m-64 experiment. That is because pedestrians walking space in the 5 m experiment is less than 10 m, and the more congested situation makes pedestrians willing to directly choose a large detour during the initial period of the trip.

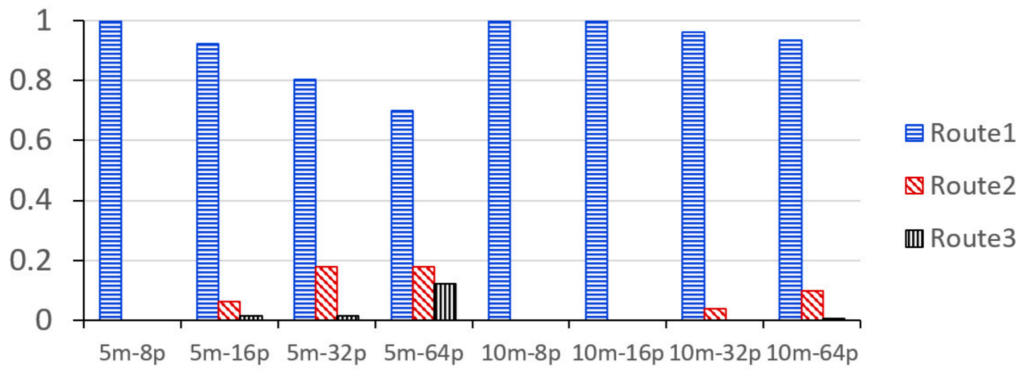

Figure 8. Comparison chart of the proportion of detour modes in each experiment.

In general, although the proportion of pedestrians choosing large detours (Route 2) significantly increases with the increase of population density, the group that chooses to repeatedly adjust the route through the conflict area (Route 1) remained the majority. On the one hand, this is because pedestrians often choose the shortest route, although they rarely realize that they are taking the minimization of distance as the main route selection strategy. On the other hand, the model in this paper starts from the circle antipode walking experiment. The participants in the experiment are young people aged 18–28, and they were in a youthful state. When facing the conflict area, they are more inclined to choose to go through the conflict area and pursue the shortest path. In the real situation, due to the influence of age, gender, physical condition, and other factors, the proportion of the group that passes through the conflict area will decrease, while the proportion of the other group that chooses large detours will increase. This also proves that it is necessary for us to consider the group that avoids the common conflict area and directly chooses large detours before walking or during the initial period of the trip.

Accordingly, the angle of large detours pedestrian deviates from the direction of the destination point is larger. Figure 9 depicts the travel angle distribution between the pedestrian walking direction and the destination point direction in each experiment.

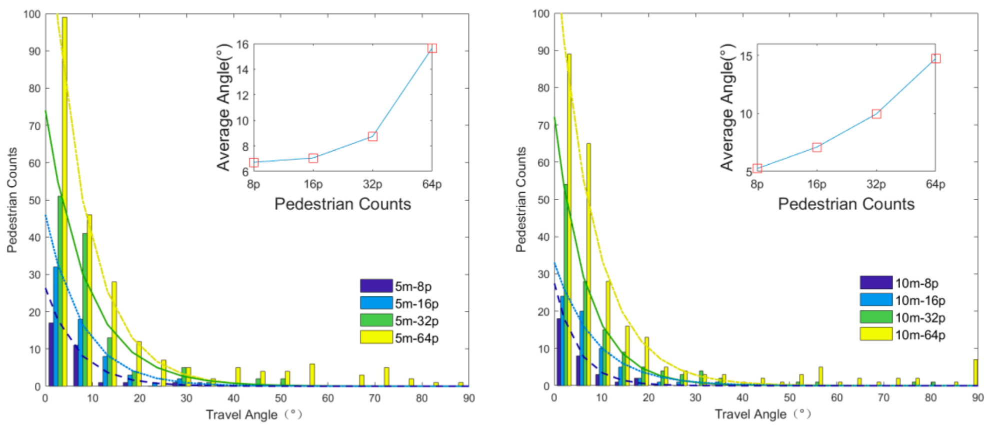

Figure 9. Pedestrian travel angle distribution.

As the number of pedestrians increases, the number of large detour pedestrians also increases, so the average travel angle of pedestrians increases gradually. The pedestrian counts decrease with the increase of travel angle, and the exponential distribution is introduced for fitting. Similarly, when p-value is greater than 0.05, it indicates that the travel angle follows the exponential distribution, and the p-value indicates that it has a good fitting effect, as shown in Table 2. Note that the 64p experiment does not conform to the exponential distribution. This is because pedestrians are too dense, and the detour angle of pedestrians will be seriously tailed, even some angles greater than 90°.

Table 2. The *p*-value of pedestrian travel angle.

Experiment	*p*-Value			
	8p	**16p**	**32p**	**64p**
5 m	0.2536	0.4734	0.3045	0
10 m	0.6189	0.6992	0.1688	0

4. Simulation Experiment

In this section, different pedestrian dynamics models, namely traditional SFM, double-layer decision model, and the extended SFM proposed in this paper are used to simulate and analyze the circle antipode walking experiment, and then compared with the experimental data to study the performance of the extended SFM. Section 4.1 describes the parameter setting and simulation results of each model; Section 4.2 uses relevant indicators to evaluate the extended SFM.

4.1. Parameter Setting and Simulation Results

At the strategy level, this paper uses the maximum likelihood estimation method to calculate the parameters a, b_1, and b_2 of logit models, as shown in Table 3, so the equation of Logit model is expressed as follows:

$$p_i = \frac{\exp(-6.613 + 0.189 \cdot X_1 + 0.228 \cdot X_2)}{1 + \exp(-6.613 + 0.189 \cdot X_1 + 0.228 \cdot X_2)} \tag{25}$$

Table 3. Logit parameter estimation results.

Independent Variables	B	S.E.	Wald	Sig.	Exp(B)
Detour angle b_1	0.189	0.063	9.085	0.000	1.208
Starting time b_2	0.228	0.057	16.093	0.000	1.256
Constant a	−6.613	1.346	24.136	0.000	0.001

Note: B: estimated value of constant term and partial regression coefficient; S.E.: standard error; Wald: chi-square value used to test the B; Sig.: significance; Exp(B): OR value.

The Sig. values are less than 0.05, indicating that the independent variable has a significant impact on the choice of pedestrian detour mode. This is the reason why this paper selects the two parameters: starting time and detour angle. At the same time, the Exp(B) values of the two parameters are 1.208 and 1.206 respectively, both greater than 1, indicating that the larger the starting time and detour angle of pedestrians, the higher the probability of choosing a large detour.

At the tactical level, the predicted visual perception density is used to guide the decision-making of detour points, and the relevant parameters are consistent with the papers of Li et al. [21]. The visual angle is $[-60^{\circ}, 60^{\circ}]$. k_2 is calculated by the detour level and the distance from the starting point l, i.e., $k_2 = \frac{exprnd(\mu_D)}{l/4+1}$. Detour level obeys the exponential distribution of parameter μ_D. The maximum instantaneous speed of the pedestrian in the quarter motion cycle is defined as the desired speed. It is verified that the desired speed of pedestrians follows a log-normal distribution with a mean of 0.9267 and a variance of 0.2767. For the group that repeatedly adjusts routes during the trip, the minimum travel cost is used to determine the optimal path point. For the group which has pre-planned the route before the travel or during the initial period of the trip, two heuristic rules are used to guide the decision-making of detour points. The parameter settings in tactical layer are shown in Table 4.

Table 4. Model parameter.

Parameter	Value	Parameter	Value
L	8 m	M	12
μ_D	1.58953	δ	0.004
m_i	$[65, 90]$ kg	τ_i	0.29 s
α	0.26	β	2.78
k_1	1	k_2	Determined by μ_D

At the operational level, the Voronoi-based SFM is used to deal with the temporary conflict in the process of moving toward the detour point, and the relevant parameters are consistent with the papers of Helbing D. [8].

Figure 10a shows the pedestrian trajectory and rotation trajectory in the first experiment of 5m-32p. The rotation trajectory is to rotate all pedestrian tracks to the same starting point and ending point, see Equation (18). Taking this experiment as the simulation object, traditional SFM, double-layer decision model, and the extended SFM are used for simulation, as shown in Figure 10b–d. Comparing the experiment and the simulation diagrams, we can see that the previous pedestrian detour models do not reflect the feature that pedestrians directly choose a large detour before departure or during the initial period of the trip, resulting in an obvious increase in the mean local density of pedestrian trajectory.

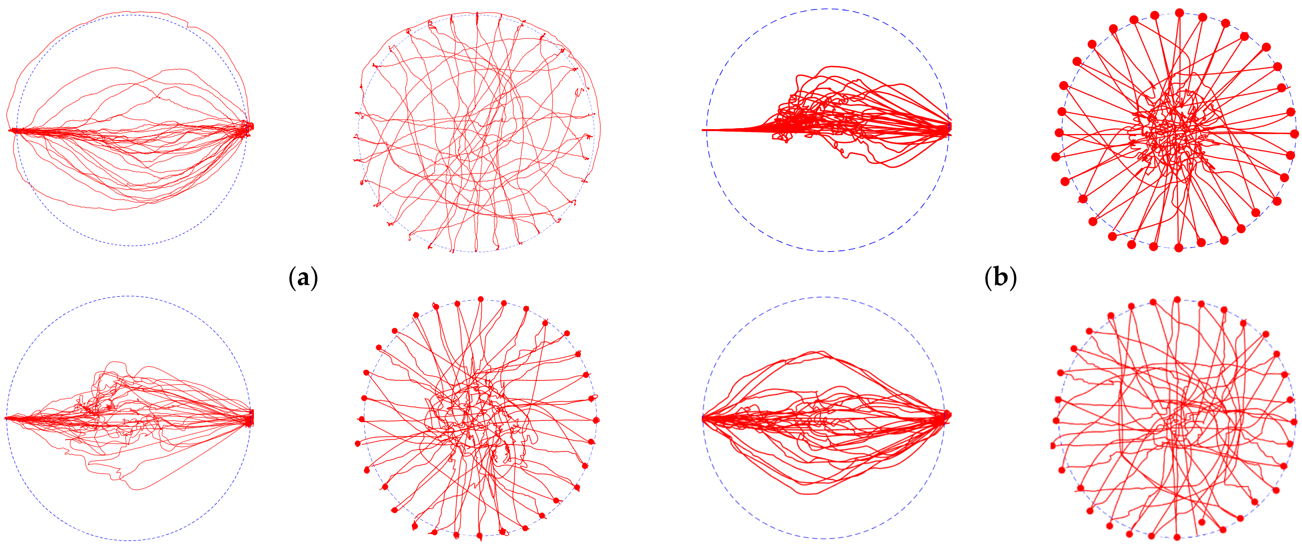

(**a**) (**b**) (**c**) (**d**)

Figure 10. Trajectory and rotation trajectory of each model compared to the walking experiment. (**a**) Experiment, (**b**) traditional SFM, (**c**) double-layer decision model, (**d**) extended SFM.

4.2. Model Evaluation

Generally speaking, there are three main methods to verify pedestrian dynamic models: ① the fundamental diagram [31,33]; ② observation data (e.g., trajectory and statistical characteristics) [34]; ③ self-organized phenomena (e.g., arching formation and stripe formation) [35]. In this study, in order to reflect detour decision-making, conflict avoidance, and other crucial motion characteristics, we choose trajectory data and some statistical indexes to intuitively show pedestrian detour behavior. For trajectory, it can show the spatial distribution density of pedestrians and the flow on different walking paths. For statistical indexes, it can quantitatively reflect the characteristics of the walking trajectory. In addition, pedestrians will make different choices when facing the conflict area in the central area in the experiment. To measure this feature, the density of the population was calculated.

Usually, K-S test is used to test the similarity of two samples, and DTW method is used to test the similarity of two sequences. Therefore, the travel time, route length, and detour level are tested by K-S test. Similarly, the DTW method is applied for mean local density and central density. Equations (25) and (26) are used to standardize the results obtained by the K-S test and DTW method, as shown in Figure 11.

$$S_D = 1/\left(1 - \log_{10} p\right) \tag{26}$$

$$S_T = 1/\left(1 + \log_{10}(1 + DTW)\right) \tag{27}$$

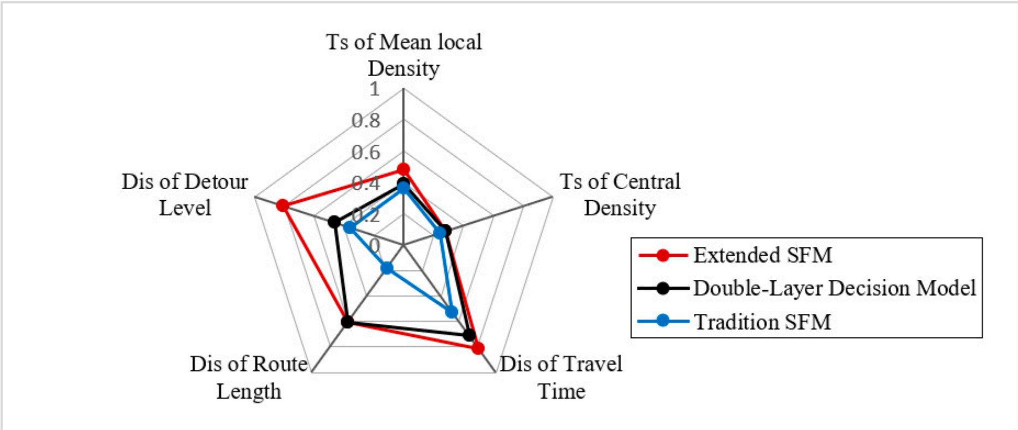

Figure 11. Comparison chart of model index scores.

The expanded SFM performs well in the five distribution indexes. As can be seen from Figure 11, the scores of the five indexes are 0.81 (detour level), 0.48 (mean local density), 0.28 (central density), 0.81 (travel time), and 0.61 (route length). In particular, the indexes of detour level, mean local density and travel time are significantly better than the double-layer detour decision model and traditional SFM.

The trajectory diagram and the index score results show that the extended SFM can well reproduce the trajectory in the circle antipode walking experiment. This is because the model divides pedestrians into two groups: "repeatedly adjusting the route during the trip" and "pre-planning the route before walking or during the initial period of the trip" at the strategic level. The latter directly chooses a large detour to avoid the conflict in the central area. The reduction of the number of pedestrians in the former leads to less conflict, and accordingly, shorter travel time and lower pedestrian density. This is more in line with the detour of the experiment. Whereas previous detour models do not consider that some pedestrians will choose large detours according to the pre-planned route. When the population density is high, the applicability of the double-layer decision model will be reduced.

5. Conclusions

The previous detour behavior modeling work only described the detour decision of pedestrians repeatedly adjusting routes during the trip, without considering that some pedestrians have pre-planned their routes before walking or in the first period of time, which led to the obvious high pedestrian density in the simulation. To improve the simulation method of pedestrian detour decisions, this paper establishes an extended SFM model based on the three-level framework of pedestrian simulation proposed by Hoogendoorn and Bovy [13]. In this model, the two groups of "repeatedly adjusting the route during the trip" and "pre-planning the route before walking or during the initial period of the trip" are separated at the strategy level, so as to give tactical guidance to the two groups respectively. At the tactical level, for the latter, two simple heuristic rules are used to guide its detour direction, while for the former, the perceived density in the visual field is used to determine the detour direction. At the operational level, Voronoi-based SFM is used to cope with the direct conflicts to the detour direction at the tactical level.

Compared with the traditional SFM and the double-layer decision model, the extended SFM proposed in this paper describes the detour characteristics of the two groups in the circle antipode walking experiment in more detail. The simulation trajectory and the index score show that both the original trajectory and the rotation trajectory are better than the above models.

However, this paper still has the following limitations:

(1) In reality, pedestrians may switch or combine the two movement modes of "repeatedly adjusting the route during the trip" and "pre-planning the route before walking or during the first period of the trip", which is not considered in this paper. In the future, we will continue to explore whether the path decision-making modes of pedestrians have changed in the process of moving from one place to another, which has not received much attention so far.

(2) Pedestrians are directly divided into two groups at the starting position for different walking guidance, without considering the dynamic time difference of pedestrians making this large-scale detour decision. In fact, this decision is made before the trip or during the initial period of the trip, and there is a certain time difference.

(3) In fact, the speed of movement depends on the quality of the road and the landform. The tendency of pedestrians to avoid conflict areas is related to the individual characteristics of pedestrians. In the future, we will further study the influence of road quality, terrain and individual characteristics on pedestrians' walking speed, and detour tendency.

Author Contributions: The authors confirm contribution to the paper as follows: methodology, M.L.; data curation, Q.N.; formal analysis, Q.N. and M.L.; writing—original draft preparation, Q.N.; writing—review and editing, Q.N. and M.L. All authors have read and agreed to the published version of the manuscript.

Funding: This research received no external funding.

Institutional Review Board Statement: Not applicable.

Informed Consent Statement: Not applicable.

Data Availability Statement: Not applicable.

Conflicts of Interest: The authors declare no conflict of interest.

References

1. Saadatseresht, M.; Mansourian, A.; Taleai, M. Evacuation planning using multiobjective evolutionary optimization approach. *Eur. J. Oper. Res.* **2009**, *198*, 305–314. [CrossRef]
2. Yang, L.; Ping, R.; Zhu, K.; Liu, S.; Xin, Z. Observation study of pedestrian flow on staircases with different dimensions under normal and emergency conditions. *Saf. Sci.* **2012**, *50*, 1173–1179. [CrossRef]
3. Hughes, R.L. A continuum theory for the flow of pedestrians. *Transp. Res. Part B Methodol.* **2002**, *36*, 507–535. [CrossRef]
4. Dressler, D.; Gro, M.; Kappmeier, J.P.; Kelter, T.; Kulbatzki, J.; Plümpe, D.; Schlechter, G.; Schmidt, M.; Skutella, M.; Temme, S. On the use of network flow techniques for assigning evacuees to exits. *Procedia Eng.* **2010**, *3*, 205–215. [CrossRef]
5. Abdelghany, A.; Abdelghany, K.; Mahmassani, H. A hybrid simulation-assignment modeling framework for crowd dynamics in large-scale pedestrian facilities. *Transp. Res. Part A Policy Pract.* **2016**, *86*, 159–176. [CrossRef]
6. Blue, V.J.; Adler, J.L. Cellular automata microsimulation for modeling bi-directional pedestrian walkways. *Transp. Res. Part B Methodol.* **2001**, *35*, 293–312. [CrossRef]
7. Zhou, X.M.; Hu, J.J.; Ji, X.F.; Xiao, X.Z.Y. Cellular automaton simulation of pedestrian flow considering vision and multi-velocity. *Phys. A Stat. Mech. Appl.* **2019**, *514*, 982–992. [CrossRef]
8. Helbing, D. Social force model for pedestrian dynamics. *Phys. Rev. E* **1995**, *51*, 4282. [CrossRef]
9. Haghani, M.; Sarvi, M. Simulating pedestrian flow through narrow exits. *Phys. Lett. A* **2019**, *383*, 110–120. [CrossRef]
10. Fiorini, P.; Shiller, Z. Motion Planning in Dynamic Environments Using Velocity Obstacles. *Int. J. Robot. Res.* **1998**, *17*, 760–772. [CrossRef]
11. Masood, K.; Molfino, R.; Zoppi, M. Simulated Sensor Based Strategies for Obstacle Avoidance Using Velocity Profiling for Autonomous Vehicle FURBOT. *Electronics* **2020**, *9*, 883. [CrossRef]
12. Antonini, G.; Bierlaire, M.; Weber, M. Discrete choice models of pedestrian walking behavior. *Transp. Res. Part B Methodol.* **2006**, *40*, 667–687. [CrossRef]

13. Hoogendoorn, S.P.; Bovy, P.H.L. Pedestrian route-choice and activity scheduling theory and models. *Transp. Res. Part B Methodol.* **2004**, *38*, 169–190. [CrossRef]
14. Farina, F.; Fontanelli, D.; Garulli, A.; Giannitrapani, A.; Prattichizzo, D. Walking Ahead: The Headed Social Force Model. *PLoS ONE* **2017**, *12*, e0169734. [CrossRef] [PubMed]
15. Li, W.; Gong, J.; Yu, P.; Shen, S.; Li, R.; Duan, Q. Simulation and analysis of congestion risk during escalator transfers using a modified social force model. *Phys. A Stat. Mech. Appl.* **2015**, *420*, 28–40. [CrossRef]
16. Moussaid, M.; Helbing, D.; Theraulaz, G. How simple rules determine pedestrian behavior and crowd disasters. *Proc. Natl. Acad. Sci. USA* **2011**, *108*, 6884–6888. [CrossRef]
17. Yuen, J.K.K.; Lee, E.W.M. The effect of overtaking behavior on unidirectional pedestrian flow. *Saf. Sci.* **2012**, *50*, 1704–1714. [CrossRef]
18. Hoogendoorn, S.P.; Van Wageningen-Kessels, F.L.M.; Daamen, W.; Duives, D.C. Continuum modelling of pedestrian flows: From microscopic principles to self-organised macroscopic phenomen. *Phys. A Stat. Mech. Appl.* **2014**, *416*, 684–694. [CrossRef]
19. Xiao, Y.; Gao, Z.; Qu, Y.; Li, X. A pedestrian flow model considering the impact of local density: Voronoi diagram based heuristics approach. *Transp. Res. Part C Emerg. Technol.* **2016**, *68*, 566–580. [CrossRef]
20. Qu, Y.; Xiao, Y.; Wu, J.; Tang, T.; Gao, Z. Modeling detour behavior of pedestrian dynamics under different conditions. *Phys. A Stat. Mech. Appl.* **2018**, *492*, 1153–1167. [CrossRef]
21. Li, M.; Shu, P.; Xiao, Y.; Wang, P. Modeling detour decision combined the tactical and operational layer based on perceived density. *Phys. A Stat. Mech. Appl.* **2021**, *574*, 126021. [CrossRef]
22. Guo, N.; Hao, Q.-Y.; Jiang, R.; Hu, M.-B.; Jia, B. Uni- and bi-directional pedestrian flow in the view-limited condition: Experiments and modeling. *Transp. Res. Part C Emerg. Technol.* **2016**, *71*, 63–85. [CrossRef]
23. Hoogendoorn, S.P.; Van Wageningen-Kessels, F.; Daamen, W.; Duives, D.C.; Sarvi, M. Continuum theory for pedestrian traffic flow: Local route choice modelling and its implications. *Transp. Res. Part C Emerg. Technol.* **2015**, *59*, 183–197. [CrossRef]
24. Abraham, J.E.; Hunt, J.D. Random utility location, production, and exchange choice; Additive Logit model; and spatial choice microsimulations. *Transp. Res. Rec.* **2007**, *2003*, 1–6. [CrossRef]
25. Park, B.U.; Simar, L.; Zelenyuk, V. Nonparametric estimation of dynamic discrete choice models for time series data. *Comput. Stat. Data Anal.* **2017**, *108*, 97–120. [CrossRef]
26. Lovreglio, R.; Fonzone, A.; Dell'olio, L. A mixed logit model for predicting exit choice during building evacuations. *Transp. Res. Part A Policy Pract.* **2016**, *92*, 59–75. [CrossRef]
27. Steffen, B.; Seyfried, A. Methods for measuring pedestrian density, flow, speed and direction with minimal scatter. *Phys. A Stat. Mech. Appl.* **2010**, *389*, 1902–1910. [CrossRef]
28. Luo, L.; Liu, X.B.; Fu, Z.J.; Ma, J.; Liu, F.X. Modeling following behavior and right-side-preference in multidirectional pedestrian flows by modified FFCA. *Phys. A Stat. Mech. Appl.* **2020**, *550*, 124149. [CrossRef]
29. Ling, H.; Wong, S.C.; Zhang, M.; Shu, C.W.; Lam, W. Revisiting Hughes' dynamic continuum model for pedestrian flow and the development of an efficient solution algorithm. *Transp. Res. Part B* **2009**, *43*, 127–141.
30. Kretz, T.; Lehmann, K.; Hofs, I.; Leonhardt, A. Dynamic Assignment in Microsimulations of Pedestrians. *arXiv* **2014**, arXiv:1401.1308.
31. Parisi, D.R.; Gilman, M.; Moldovan, H. A modification of the Social Force Model can reproduce experimental data of pedestrian flows in normal conditions. *Phys. A Stat. Mech. Appl.* **2009**, *388*, 3600–3608. [CrossRef]
32. Xiao, Y.; Gao, Z.; Jiang, R.; Li, X.; Qu, Y.; Huang, Q. Investigation of pedestrian dynamics in circle antipode experiments: Analysis and model evaluation with macroscopic indexes. *Transp. Res. Part C Emerg. Technol.* **2019**, *103*, 174–193. [CrossRef]
33. Huang, S.S.; Wei, R.C.; Lo, S.M.; Lu, S.X.; Li, C.H.; An, C.; Liu, X.X. Experimental study on one-dimensional movement of luggage-laden pedestrian. *Phys. A Stat. Mech. Appl.* **2019**, *516*, 520–528. [CrossRef]
34. Bera, A.; Kim, S.; Manocha, D. Online parameter learning for data-driven crowd simulation and content generation. *Comput. Graph.* **2016**, *55*, 68–79. [CrossRef]
35. Helbing, D.; Buzna, L.; Johansson, A.; Werner, T. Self-organized pedestrian crowd dynamics: Experiments, simulations, and design solutions. *Transp. Sci.* **2005**, *39*, 1–24. [CrossRef]